DESIGN OF A HYBRID ELECTRIC PROUPULSION SYSTEM WITHIN A PRELIMINARY AIRCRAFT DESIGN SOFTWARE ENVIRONMENT

B. Aigner, M. Nollmann, E. Stumpf
Institute of Aerospace Systems, RWTH Aachen University
Wüllnerstr. 7, 52062 Aachen

ABSTRACT

The ambitious climate objectives set by the European Commission within the scope of ACARE Flight Path 2050 call for significant improvements in terms of efficiency for future aircraft configurations [1]. One of the main drivers for these improvements is the development of novel propulsion systems. Therefore, stakeholders in the aviation sector are increasingly interested in electric propulsion concepts, due to higher efficiency and reduction of local emissions. While in small aircraft for general aviation applications (CS-23) full electric propulsion concepts seem realistic for medium-term applications, in the field of large aircraft (CS-25) these concepts are not feasible in a 2030-2050 timeframe. By contrast, hybrid electric propulsion concepts are scalable with regard to flight range and payload and are considered to achieve similar operational flexibility as present-day conventional technologies. Thus, a variety of hybrid electric propulsion technologies has been investigated within preliminary aircraft design research projects in recent years.
Within the scope of the presented research, a design methodology has been implemented into the aircraft design suite MICADO (Multidisciplinary Integrated Conceptual Aircraft Design and Optimization Environment) to evaluate electric propulsion concepts on a preliminary level in a short time and with the necessary flexibility to investigate a broad design space. As a first approach, the concept of an uncoupled parallel hybrid electric propulsion system, consisting of two gas turbine engines and two electrically driven ducted fans powered by batteries, has been chosen and integrated into an Airbus A320-200 aircraft.
Preliminary results have shown a block fuel reduction only for design ranges below 900 NM depending on the conducting material. In consideration of realistic assumptions for specific battery weights, a mission energy (or even cost) reduction cannot be achieved yet, which is in line with research findings from other organizations. Therefore, further studies considering improvements such as a more feasible aircraft configuration, different propulsion system architectures and variable degrees of hybridization throughout the flight mission are planned for future research work.

KEYWORDS

Hybrid electric propulsion, Aircraft design, MICADO

1. INTRODUCTION

For almost ten years, the Institute of Aerospace Systems (ILR) at RWTH Aachen University has been continuously developing the preliminary aircraft design software MICADO (Multidisciplinary Integrated Conceptual Aircraft Design and Optimization Environment) [2]. MICADO enables automated aircraft design, operational studies, as well as technology integration and assessment. Its modular program structure allows for exchangeability and extensibility of the integrated design and analysis programs. The focus of this paper is set on the implementation of a design methodology for hybrid electric propulsion systems into the software environment. In order to clarify further research priorities, it is particularly important to determine a feasible propulsion concept and the impact of the new system components on the overall aircraft. Since a variety of such propulsion concepts have been introduced and discussed in the field, in a first step, an overview on (hybrid) electric propulsion concepts is given. Secondly, a feasible concept is selected and described in more detail with respect to its general layout and its implementation into MICADO.

doi:10.25967/480153

2. ELECTRIC PROPULSION ARCHITECTURE SELECTION

Over the past years, electric propulsion concepts have increasingly become a focus in the aviation sector when considering ecological efficiency. Boeing [3], Airbus [4], as well as research organizations such as Bauhaus Luftfahrt [5-10], the German Aerospace Center (DLR), and different universities have carried out studies within the field. Generally, one can subdivide electric propulsion into three main areas:

- All electric propulsion
- Turboelectric propulsion
- Hybrid electric propulsion

The main advantages of all electric propulsion are its overall efficiency (on aircraft level) of more than 90% and practically zero local emissions throughout the flight mission [11]. However, even with optimistic forecasts of battery technology development, these concepts are only feasible for small aircraft, as shown in various studies [5, 12, 13]. In the field of large commercial airplanes (CS-25), the all-electric concept is hardly realizable in a 2030-2050 timeframe.

In turboelectric propulsion concepts, one or more combustion engines (e.g. gas turbines) provide the necessary power for electrically powered engines using generators for a transformation of the mechanical into electric power. The basic idea is for the combustion engines to operate close to optimum efficiency. The approach was applied in different research projects such as NASA NX-3, ESAero Eco-150 or NASA STARC-ABL [14-16].

A combination of the two aforementioned electrical propulsion concepts is hybrid electric propulsion. In principle, two different hybrid electric propulsion concepts can be distinguished: series and parallel hybrid.

In a series hybrid, the propulsive power is provided by an electric source (e.g. battery) and / or a generator powered by a combustion engine (see Fig. 1).

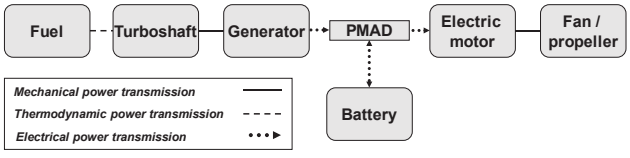

Fig. 1: Series hybrid electric propulsion architecture

The electric power from batteries or generators is transferred to the engines via a power management and distribution system (PMAD). Various architecture variations are possible, e.g. recharging the batteries during flight phases with lower power requirements (e.g. steady cruise flight) . One of the main advantages of a series architecture is an improvement of efficiency, because the combustion engine is decoupled from direct thrust generation. Therefore, it can operate at an optimum design point. Another advantage is the ability to distribute the electrical engines along the aircraft (distributed electric propulsion, DEP), increasing overall efficiency. Due to scalability problems, this is not as easily realizable with combustion engines. The DEP approach, for example, was pursued by Airbus in the E-Thrust project using several electrically powered fans along the wing and a gas turbine as main power source in the rear fuselage [4]. In the CS-23 sector, NASA investigated distributed electric high-lift propellers on the wing to provide the required lift for low-speed and therefore, enabling an optimized wing design for cruise conditions instead of low-speed requirements [17]. The European projects DisPURSAL [9] and CENTRELINE [10], as well as the NASA STARC-ABL project [16] investigate the so-called propulsive fuselage as a distributed propulsion concept using synergies between the electrification of the propulsion and an increase of aerodynamic efficiency due to fuselage wake-filling.

Another possibility for hybrid electric propulsion is the parallel architecture (see Fig. 2).

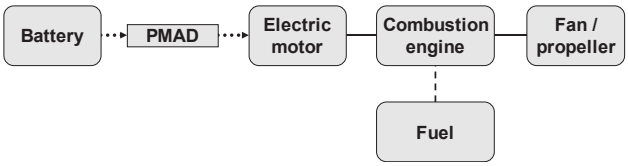

Fig. 2: Parallel hybrid electric propulsion architecture

In this concept, the electric motor is mounted on one shaft together with a combustion engine (possible gearbox in between). Both engine types can be operated simultaneously or separately. The electric engine can also be used to compensate for peak loads in flight segments with high power requirements (e.g. takeoff), while the combustion engine is sized for an optimum design point (e.g. cruise flight). Pornet et al., who developed a sizing and performance assessment methodology for large commercial aircraft with hybrid electric propulsion, for instance, investigated parallel architectures within the scope of a research project at Bauhaus Luftfahrt. On a 900 NM flight mission an overall block fuel reduction of 13% was achieved assuming a specific battery energy density of 1500 Wh/kg [6]. Another research project worth mentioning is Boeing's Subsonic Ultra Green Aircraft Research (SUGAR), in which a parallel hybrid electric propulsion system was integrated in the so-called SUGAR Volt configuration. The overall fuel consumption on a 900 NM mission could be reduced by over 60% assuming a battery energy density of 750 Wh/kg [3]. Despite the promising results achieved in previous research projects, the parallel hybrid electric propulsion concept has one major drawback. Due to the fact that the electric motor and gas turbine run on a common shaft, there is the risk of a shift of the gas turbine's operation line, which can lead to part-loading and

therefore decrease efficiency. The operation line shift can even become critical with respect to the surge line margin of the gas turbine [7]. This means that the concept is difficult to apply for retro-fit designs of already existing aircraft, because the gas turbine would have to be completely redesigned together with the electric engine.

In addition to the above-mentioned two main categories (series & parallel) for hybrid electric propulsion, it is also possible to combine these two basic concepts. Pornet et al., for example, introduced a distributed parallel architecture, which is a mixed concept of both basic arrangements [7]. The layout is displayed in Fig. 3.

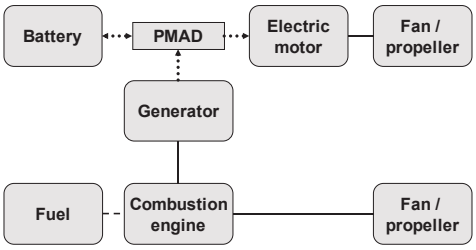

Fig. 3: Distributed parallel hybrid architecture

As in the basic parallel layout, both engine types, combustion engine and electric motor provide the required thrust for the aircraft. However, they are completely mechanically decoupled from each other. Optionally, an additional generator can be applied either to charge the batteries or to directly power the electric motor. Due to decoupling of the two engine types this architecture can be used for retro-fit designs of already existing aircraft. In the studies by Pornet et al., a narrow body aircraft was equipped with two geared turbofans and two electric fans. Assuming a battery energy density of 1000 Wh/kg a fuel reduction was achieved starting from flight distances of 1100 NM downwards [7].

From the short overview of electric propulsion concepts given above, it can be concluded that various options to electrify large commercial aircraft exist. Selecting a suitable concept strongly depends on the use-case of the aircraft to design. Depending on the top level aircraft requirements (TLAR), such as design range, cruise Mach number, and number of passengers, the final system architecture can vary considerably. Since the main purpose of this research is to find a suitable electric propulsion architecture as a starting point for an implementation into the ILR in-house aircraft design software MICADO, the simplicity of the software integration additionally plays a large role in the selection.

Within the scope of this research, it was concluded to integrate the distributed parallel hybrid architecture displayed in Fig. 3, due to various reasons explained hereafter.

1. The distributed parallel architecture is expected to reduce carbon dioxide (CO^2) emissions for flight distances below 1100 NM. A decrease of the design flight range is usually a required factor to obtain block fuel improvements when integrating electric propulsion on CS-25 type aircraft due to the increased overall system weight. However, a reduction of the range can be considered feasible when looking at studies on aircraft operations. These studies show that 88-90% of all flights in Europe and Asia are below a distance of 1000 NM. In the United States, 90% of the domestic flights are within a range of 1650 NM [18]. Nevertheless, one has to keep in mind that a reduced flight range also decreases operational flexibility, which can be a decisive factor in an airline's purchase decision.
2. The architecture is well suitable for a retrofit design of already existing aircraft. With the largely unchanged gas turbine, which is decoupled from the electric motors, the concept can be applied as a midterm solution. Therefore, it would be possible to gain initial experience with hybrid electric propulsion technologies in flight operations, before moving to more sophisticated architectures such as distributed series hybrid electric propulsion.
3. The integration of electric propulsion systems into the aircraft design software MICADO calls for significant changes in the underlying software architecture. Therefore, a concept that is relatively simple to integrate into the software environment is desirable for an initial approach. In contrast to most of the other architectures presented, the distributed parallel concept meets these requirements.

Finally, It can be concluded that the distributed parallel hybrid electric propulsion concept represents a good compromise between the capability of a retrofit design and a potential block fuel reduction, although it is not the one with the highest CO^2 reduction potential or most synergies (e.g. distributed electric propulsion). Therefore, it is selected for implementation into the ILR software environment presented within the scope of this paper. Additionally, it should be noted that instead of batteries, fuel cells could have been chosen as the primary energy source for the electric powertrain. However, in order to keep the complexity as low as possible at the moment, fuel cells are not investigated within this paper.

3. HYBRID ELECTRIC PROPULSION SIZING METHODOLOGY

In the presented work, the distributed parallel hybrid electric propulsion architecture was integrated as a retrofit design on an Airbus A320-200 aircraft. Fig. 4 shows the overall system layout of the concept.

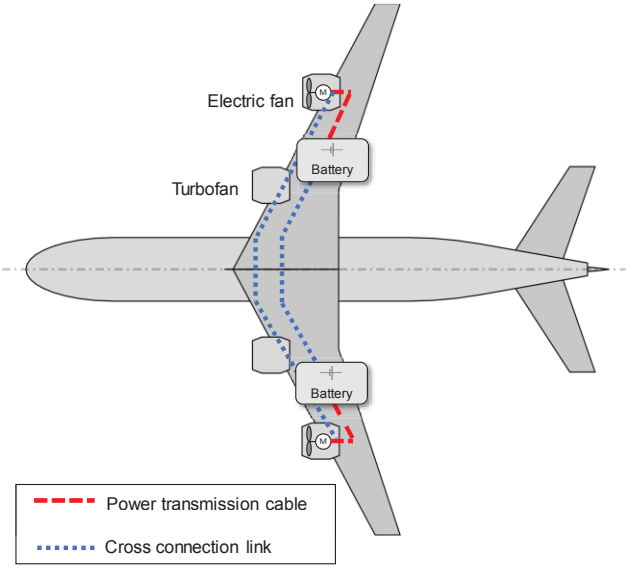

Fig. 4: Overall system layout with batteries installed in the wings

Depending on the degree of hybridization, the batteries can either be integrated into the fuselage with fuel tanks in the wing, or the other way around, depending on the available space. In this context, the degree of hybridization H_T represents the amount of thrust provided by the electric fans ($T_{SLST,electric}$) compared to the total installed thrust of the aircraft ($T_{SLST,total}$).

$$H_T = \frac{T_{SLST,electric}}{T_{SLST,total}} \quad (1)$$

Fig. 5 provides a more detailed overview on the hybrid electric powertrain with respect to the associated component efficiencies.

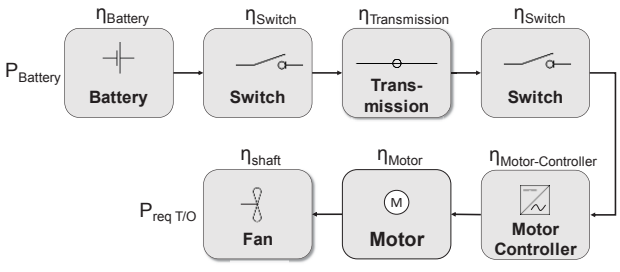

Fig. 5: Electric powertrain efficiency chain

The overall efficiency η_{total} of the electric powertrain is given as the multiplication of the component efficiencies

$$\eta_{total} = \prod_{i=0}^{N} \eta_i \quad (2)$$

where the η_i is the efficiency of each individual component, e.g. fan, motor, battery, and transmission. Hereafter, the sizing methodologies for the individual components of the electric powertrain are explained. The turbofan engine powertrain is not presented in detail, since it is completely identical to a conventional turbofan propulsion system.

3.1. Battery

One of the key elements in the electric powertrain is the storage of the electric energy. The most challenging factors for future electric air mobility are the specific energy density in [Wh/kg] (defined as the ratio between the amount of stored energy and the mass of the battery) and the specific power density in [W/kg] (defined as the ratio between maximum output power and the battery mass). Current state-of-the-art lithium-ion batteries have a maximum energy density of 240-270 Wh/kg [19], which is more than a factor of 40 times less than kerosene (12000 Wh/kg) [20] and is not sufficient for large commercial aircraft applications [12]. Therefore, current research activities in the field of battery technology are aiming towards new battery materials with a higher specific energy density. Lithium-air batteries have the highest potential with respect to energy density with a theoretical value of 3450 Wh/kg on the material side. This value can however not be achieved in real applications. A recent survey by the Fraunhofer Institute for system and innovation research predicts a possible energy density of up to 1000 Wh/kg for the future, while 800 Wh/kg on cell level and 500 Wh/kg on pack level have already been demonstrated for military applications [19, 21]. Current bottlenecks with the technology are the low power density, problems with contamination of the cells caused by the use of air, and problems with rechargeability. Another promising battery technology are lithium-sulfur cells. The predicted maximum energy density of these cells is however lower than for lithium-air cells, with an approximate of 600 Wh/kg [19]. Similar to lithium-air cells, the current power density is too low for aviation applications, which calls for further research on the technology. Generally, all state-of-the-art battery technologies are inapplicable for the use-case presented in this work. Nevertheless, since the target timeframe of the research is 2030-2050, it is assumed, that battery technology will be further developed, so that it can be utilized for aviation applications in the future. The above-mentioned predicted specific energy densities of lithium-air batteries are therefore assumed hereafter taking into account different scenarios, ranging between 500 Wh/kg and 1500 Wh/kg.

3.2. Power transmission

Transmission of the required power from the batteries to the electric engines is another main challenge for electric propulsion architectures. As it is already pursued in state-of-the-art aircraft (e.g. Boeing 787), a direct current (DC) power distribution is chosen. This leads to a weight reduction as the number of cables can be reduced compared to a 3-phase alternate current (AC) system. Consequently, for electric consumers, which require AC, additional converters have to be installed. Due to the high power requirements in the double-digit megawatt range, conventional conductors (copper, aluminum) might not be feasible range for the presented use-case. Hence, in addition to conventional cable technologies, high-temperature superconductors (HTS) are also investigated below.

3.2.1. Conventional power transmission

In today's aircraft, either copper or aluminum conductors are used for electric power transmission. The main differences between the two materials are their conductivity (copper: $\sigma_{copp} = 59 \frac{S}{mm^2} m$, aluminum: $\sigma_{alu} = 36 \frac{S}{mm^2} m$) and gravimetric density (copper: $\rho_{copp} = 8.9 \frac{g}{cm^3}$, aluminum: $\rho_{alu} = 2.7 \frac{g}{cm^3}$). An investigation on the materials based on the tradeoff between conductivity (efficiency) and density (mass) on overall aircraft level is presented in chapter 5.1 of this work.

The design of the conventional conductors is performed using methodologies by Stückl [22] and Kasikci [23]. In the first step of the sizing process, the required cross section of the conducting material is calculated taking into account a degradation of the conductivity due to the flight altitude. Additionally, isolation with cross-linked polyethylene and sheath is required. Therefore, the total cable mass is calculated as

$$m_{cable} = m_{conductor} + m_{isolation} + m_{sheath}, \quad (3)$$

with

$$m_{conductor} = \rho_{conductor} \cdot A_{req} \cdot l_{cable}, \quad (4)$$

$$m_{isolation} = t_{isolation} \cdot \rho_{isolation} \cdot c_{conductor} \cdot l_{cable} \quad (5)$$

and

$$m_{sheath} = t_{sheath} \cdot \rho_{sheath} \cdot c_{isolation} \cdot l_{cable}, \quad (6)$$

where $t_{isolation}$ and t_{sheath} are the required thickness for isolation and sheath adopted from Stückl's method based on DIN VDE 0276 603, DIN VDE 0276 620 and DIN 50264 [22].

3.2.2. Superconducting power transmission

Due to high power requirements, superconductors have become the focus when considering electric propulsion for large aircraft. The main advantage of superconductors is the loss of ohmic resistance below a certain cryogenic temperature. Based on the critical temperature, a distinction is made between high- (> 30 K) and low-temperature superconductors (< 30 K). High-temperature super-conductors (HTS) are usually preferred due to the lower requirement for cooling. In the past decades, different superconducting materials have been investigated. Yttrium barium copper oxide (YBCO) has a very high potential for most applications, because of its critical temperature of 92 K, which is above the boiling temperature of liquid hydrogen (77 K). Previous studies on superconducting applications reached specific cable masses between 9.8 kg/m [24] and 13 kg/m [25]. To make the technology applicable for aircraft applications, the focus of future developments has to be set on the optimization of the specific weight for HTS cables. Brown et al. predicted a specific mass of 5 kg/m for aircraft applications in the future, which is adopted for the work performed in this paper. The efficiency of the superconductors is assumed to 99.99% due to the almost neglectable ohmic resistance. However, to keep the temperature at the required level, an additional cooling system is needed. The thermal losses, according to Haugan et al. [26] can be calculated with

$$Q_{thermal} = (0.45 \cdot n_{cond} \cdot I_{cond} + 200) + 0.5 \cdot l_{cond}, \quad (7)$$

The thermal heat $Q_{thermal}$ is the main input parameter for the design of the cryogenic cooling system, which is described in section 3.7.

3.3. Switches

In contrast to low-power loads, where simple mechanical relays are sufficient, the switching and protection of high-voltage and high power loads call for more complex components. The mechanical separation of two high-power conductors would lead to a conducting plasma arc under certain conditions, causing damage of the conductors. Additionally, according to Paschen's law the electric arcing becomes more critical as the air density drops with rising altitude. Therefore, for the presented electric powertrain, solid state power controllers (SSPC) are considered. They provide an additional protection of the loads and align switching between the individual circuits. Different types of SSPC exist, such as metal-oxide-semiconductor field-effect transistors (MOSFET), insulated-gate bipolar transistors (IGBT), and thyristor transistors. Within the scope of this work, the IGBT with a maximum blocking voltage of 7500 kV is chosen. Stückl derived a linearized weight trend to account for the IGBT mass from state-of-the art IGBTs, which is adopted here

$$m_{switch}[kg] = 1.6 \cdot 10^{-4} \cdot P_{switch}[kW] + 0.6 \quad (8)$$

where $P_{switch}[kW]$ is the maximum electrical power in the powertrain system [22]. The IGBT's efficiency can be estimated with the associated voltage drop, which depends on the blocking voltage. For the calculation, again a linearized correlation by Stückl is used [22]

$$U_{CE,sat}[V] = 4.3 \cdot 10^{-4} \cdot U_{block}[V] + 1.4 \quad (9)$$

Finally, the efficiency for the IGBT switch can be calculated with

$$\eta_{switch} = 1 - \frac{U_{CE,sat} \cdot I}{P_{switch}} \quad (10)$$

with the current I and the electrical power P_{switch}.

3.4. Electric motor

The selection of a suitable electric motor for the applied concept is a very important task, mainly due to the comparatively very high power requirements. State-of-the-art conventional electric motors (e.g. asynchronous, synchronous, switch reluctance motors) achieve a specific power density of 5-10 kW/kg for peak power and about 5.5 kw/kg for continuous power [27-29], which is about half that of conventional turbofan engines. With further optimizations of the specific power density of electric motors, similar values as for a gas turbine engines are conceivable in the future. A conventional electric motor could hypothetically be scaled up to the power of an aircraft gas turbine. However, a significant issue in the scaling process would be the thermal management [30]. In general, the heat losses of the electric motor and the heat dissipation of the cooling system are in equilibrium at the maximum continuous rating of the electric motor. An increase in motor power would lead to a decreased ratio of available cooling surface to the inner motor volume, so that the heat losses and heat dissipation are no longer in equilibrium. Thus, an effective motor cooling would no longer be possible. In ground based applications this problem has been solved by reducing the current density in the windings. This, in turn, results in an increase in motor mass, which makes the concept unfeasible for aircraft applications [22]. Hence, within the context of this work, superconducting motors, as an alternative concept, are considered.

Superconducting electric motors have a high efficiency and specific power density. Due to a higher current density in the superconducting wires and the resulting reduced wire cross section, the motor mass can be decreased. Furthermore, the higher current density enables an increase in the magnetic field strength and therefore, an increase in motor torque. This again enhances motor power and specific power density compared to a conventional electric motor. On the other hand, to keep the superconducting characteristics of the motor, a cryogenic cooling system is required, decreasing the overall power density. The three most common types of HTS motors are the synchronous motor, the trapped flux motor and the fully superconducting motor. In a survey on HTS motors carried out by Stückl, the fully superconducting motor proved to have the highest potential in specific power density. This is due to the fact that for the other concepts, the superconducting technology can only be applied for the DC components, whereas the AC armature windings have to be made of conventional materials, e.g. copper or aluminum. However, it should be noted that for a realization of the fully superconducting motor, further enhancements in the cryogenic cooling system technology have to be made [22]. For the target timeframe of 2030-250, these enhancements are considered to be realistic in the presented work. Within the scope of this paper, the weight for a fully HTS motor is adopted from Stückl [22]

$$\frac{\partial}{\partial m} P_{motor,in}\left[\frac{kW}{kg}\right] = 2.63 \cdot \left(P_{motor,in}[kW]\right)^{0.277} \quad (11)$$

This weight relationship is derived from studies by Brown et al. ($P_{motor} = 4742\ kW$ and $\eta_{motor} = 99.95\%$ efficiency without cryogenic cooling [31]) and by Sivasubramaniam et al. ($P_{motor} = 5000\ kW$ and $\eta_{motor} = 98\%$, including cryogenic cooling [32]). The motor efficiency is independent of the nominal power rating and part-load operation and is presumed at 99.5%. Furthermore, the volumetric density is assumed to 1105 kg/m³ with a diameter-to-length ratio of 0.76 [22].

As already mentioned, the HTS motor requires cryogenic cooling in order to remain at a superconducting state. Similarly to the superconducting power transmission cable (see section 3.2.2), as superconducting material, YBCO is used. The motor's operation temperature ranges between 50 K and 60 K. In general, the thermal losses of HTS motors mainly consist of the active heat dissipation from the HTS windings, heat transfer in the supply cables and thermal imperfections due to heat radiation and heat conduction through the motor shaft and motor housing. Another important figure of merit for the HTS motor is the ratio between the required cryogenic cooling power ($\dot{Q}_{cryo-cooling}$) and the mechanical power output of the HTS motor (P_{motor}), called cryogenic inefficiency λ_{sc}. Radebaugh et al. predict a cryogenic inefficiency of $\lambda_{sc} = 1 \cdot 10^{-4}$ for future applications, assuming a power output of 10 MW [33].

3.5. Motor controller

To convert the direct current from the power distribution system to alternate current required by the electric motor, a motor controller is necessary. The motor controller additionally enables to operate the motor at variable desired speeds and torque moments. Due to the high power requirements in the megawatt range, the controller consists of solid state switches, resulting in a reduced mass and increased efficiency. Brown et al. achieved an efficiency of

95% and a specific power density of 3-11 W/kg. Furthermore, they predicted an increase in efficiency to 99.5% and an increase in power density to 25 kW/kg including the cryogenic cooling system in the future, which is adopted in the presented work [31].

3.6. Ducted electric fan

The ducted fan model used in the presented studies is a modification of a conventional turbofan engine, in which the core engine is replaced by an electric motor (see Fig. 6).

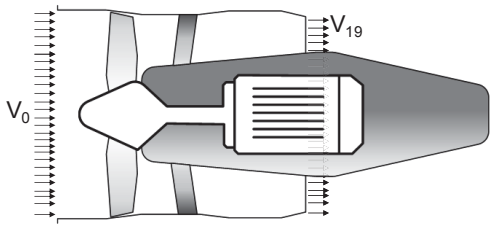

Fig. 6: Ducted fan model

The former bypass is therefore the only thrust-producing element and is completely adopted from the conventional engine. In the presented use-case, the baseline for the ducted fan model is the A320-200 engine V2527-A5 by International Aero Engines. Fan and nacelle mass are estimated with regression formulas for conventional engines from literature [2, 34]. Determining fan efficiency, on the other hand, is a more complex task. Since the fan efficiency is not a constant value, but varies at different flight altitudes and velocities, a detailed fan performance map is required. However, in the context of this work, such a performance map did not exist, yet. As a workaround, performance characteristics of the bypass of the baseline V2527-A5 engine are therefore obtained using the software GasTurb12 [35]. The authors assumed this approach feasible for an initial estimation.

3.7. Cryogenic cooling system

As already mentioned in the previous sections, a cryogenic cooling system is required to keep the superconducting state of the respective components. Today's most common cryogenic cooling technologies are Stirling-, Gifford-McMahon-, and Brayton cycles, as well as pulse tubes. The characteristic working fluids of these technologies are gases with a low boiling temperature such as hydrogen, helium, argon, nitrogen or neon. The exact selection of the used material depends on the required cooling temperature for the HTS components [22]. Stirling cycle, Gifford-McMahon cycle, and pulse tubes rely on external compressors, which are often bulky, heavy and therefore not feasible for aircraft applications. Thus, within the context of this study, the reverse-Brayton cycle cryocooler (RBCC) is used. The RBCC is considered as well suited for aircraft applications due to its scalability and reliability [36, 37].

In principle, the RBCC consists of a compressor, turbine, and heat exchangers. The present state of the art for the specific weight is around 14 kg/kW and a component efficiency of about 30% [38]. Since these RBCC are designed for ground applications, a weight optimization can be expected by new lightweight design concepts for aircraft applications. First design concepts for the aircraft application have been developed in the NASA NX-3 study. The authors predicted a specific weight of 3 kg/kW with an 30% Carnot efficiency for a RBCC [31]. In the presented work, the regression formula developed by Palmer et al. for the specific mass of an RBCC is used

$$m_{RBCC} = 27.5 \cdot P_{input} \cdot e^{-1.225\left(\log_{10} P_{input}\right)} \tag{12}$$

Where P_{input} is the required input power for the cryogenic cooling system [37]. P_{input} can be calculated with

$$P_{input} = \frac{Q}{\eta_{comp}} \cdot \epsilon \tag{13}$$

with heat load Q, component efficiency η_{comp} and Carnot efficiency ϵ as the maximum theoretic efficiency, defined as the ratio between the highest (T_{high}) and the lowest temperature (T_{low}) in the cooling process.

$$\epsilon = 1 - \frac{T_{high}}{T_{low}} \tag{14}$$

Generally, four different cryogenic cooling system architectures are possible:

- Decentralized System: Each major component is cooled by one dedicated cryocooler
- Partly decentralized System: Central cryocoolers provide a pre-coolant and local cryocoolers provide cooling to final operating temperature
- Fully centralized: One central crycooler provides a circuit of fully cooled cryogen for all components
- Open Circuit: An open circuit of expandable liquid hydrogen

A centralized cooling system is considered unsuitable in the presented use-case, because a single failure would lead to the loss of the entire cooling system. The application of an open circuit also appears unfeasible for aircraft applications, due to safety aspects. Therefore, the decentralized system and partly decentralized system are considered as appropriate. Taking into account safety aspects and due to the relatively small number of cryogenic cooling needed for the selected electric propulsion architecture, the decentralized system is selected in this study. It should be noted that for other hybrid electric architectures (e.g. with additional HTS generators and/or many HTS-motors, in consequence of distributed propulsion) the selection of the cryogenic cooling architecture has to be reinvestigated.

4. SOFTWARE IMPLEMENTATION

For implementation of the distributed hybrid electric propulsion architecture into the ILR aircraft design software MICADO, an adaption of the already existing design process is necessary. In the conventional MICADO design loop, the user has to specify the TLAR as well as configurational aspects, e.g. layout of wing and empennage. After an initial sizing (calculation of thrust-to-weight ratio, wing loading and initial guess of the maximum takeoff weight), the aircraft components including wings (main wing, horizontal and vertical tail), engines, landing gear, and on-board systems are sized. Next, the aerodynamic performance and the aircraft masses are calculated. Finally, the design mission is simulated resulting in a new maximum takeoff weight, which is converged in an iteration over the sizing process. The entire software is programmed in C++ code and uses a central XML-based data schema as an interface between different program modules, which represent the individual aircraft design disciplines. The methodologies used in MICADO will not be explained in detail here. The interested reader is referred to a publication by Risse et al. [2] for further information.

To account for hybrid electric propulsion architectures within the framework of MICADO, extensive modifications to the sizing process were necessary. The final design process is simplified in Fig. 7.

Starting with the initial sizing, the total amount of required takeoff thrust is calculated. Considering a degree of hybridization H_T specified by the user, the takeoff thrust is divided into conventionally produced thrust (turbofan engine) and electric thrust (electric ducted fans). The engine sizing scales the two engine types according to their individual thrust requirement in a so-called “rubber engine sizing”.

Subsequently, the components of the electric powertrain are designed with respect to weight and size. Since the required electric mission energy provided by the batteries is not yet known, an initial guess for the battery weight is obtained at this point. Lastly, the design mission of the aircraft is simulated in the mission analysis, assuming a degree of hybridization $H_{T,mission}$ that can differ from the one for the calculation of the required takeoff thrust within reasonable limits.

After the sizing of the aircraft components and system is finished, the design is simulated. The MICADO mission simulation divides the mission into the different segments (takeoff, climb, cruise, descent, approach, etc.), while each mission segment is again subdivided into incremental mission steps (< 1 sec). Generally, in each mission step the equations of motion are solved using the aerodynamic performance data and the current mass of the aircraft, resulting in a thrust requirement for the engines. With the hybridization factor for the mission the thrust is split between the electric fans and the turbofan engines. Additionally, the on-board system shaft power and bleed air offtakes are taken into account. The result of each mission increment is the current fuel flow from the turbofan engines as well as the required by the electrically driven fans, which is translated into required battery power by going through the electric powertrain’s efficiency chain. Fuel flow and power for each increment are integrated over the mission, resulting in required fuel mass and electric energy.

The last step of the design process is the battery sizing, where the previously obtained mission energy and an assumption for the battery specific energy density are used. Taking into account a minimum state of charge at the end of the mission, which is required for durability of the battery (e.g. 20% [39]), leads to an oversizing of the battery.

The component masses including structure, systems, engines, electric powertrain components and batteries are finally fed-back to the mass estimation module, which updates the maximum takeoff mass with respect to the initial guess value. The sizing process is repeated iteratively until the MTOW has converged.

After the convergence of the design, an off-design study can be carried out, flying at a payload/range combination different from the design point. Additionally, the degree of hybridization can be varied according to the user’s requirements.

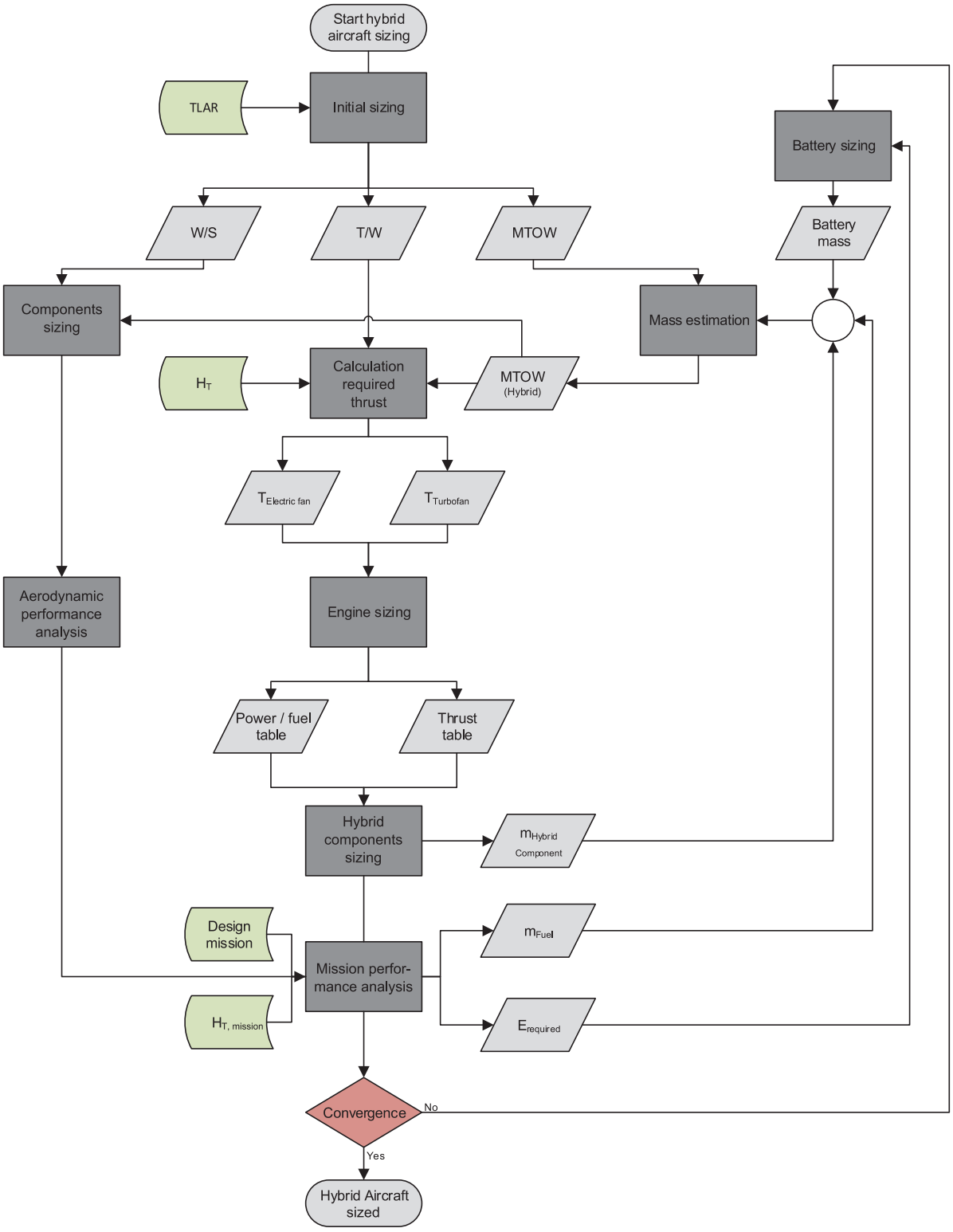

Fig. 7: Hybrid electric aircraft sizing methodology

5. STUDIES AND RESULTS

The integration of the entire electric powertrain including the individual components and their respective assumptions for specific weights, efficiencies, etc. allow for extensive studies on the applied use-case. Numerous parameters have been varied throughout the presented work to test and validate the implemented methodology. Hereafter, the most important studies and findings are presented. As previously mentioned, the baseline aircraft for the studies is a MICADO design of an Airbus A320-200.

Since the evaluation on the overall aircraft level is a multidimensional problem, it is almost impossible to grasp all influences of the design at once. Therefore, in a first step, the influence of the degree of hybridization H_T and the design range is carried out. In this study, three different conductor materials (aluminum, copper and HTS) are considered, while the assumptions for the specific components (e.g. specific energy density of the batteries) are kept constant. Secondly, a study with varied component assumptions is performed in order to explore possible feasibility limitations of the concept and to set future research perspectives.

5.1. Influence of hybridization and design range

The applied component assumptions for the presented range and hybridization studies are listed in Tab. 1 and have mainly been adopted from the findings in chapter 3.

Component	Sizing parameter	Efficiency
SSPC	$m_{SSPC} = 1.6 \cdot 10^{-4} \cdot P_{SSPC} + 0.6$	$\eta = 99.5\%$
HTS cable	$w_{cable} = 5\frac{kg}{m}$	$\eta = 99.9\%$
Motor contr.	$w_{contr.} = 15.5\frac{kg}{kW}$	$\eta = 99.5\%$
HTS Motor	$\frac{\partial}{\partial m} P_{motor,in} = 2.63 \cdot P_{motor,in}{}^{0.277}$	$\eta = 99.5\%$ $\lambda_{SC} = 10^{-4}$
Cryocooling	$m_{RBCC} = 27.5 \cdot P_{input} \cdot e^{-1.225(\log_{10} P_{input})}$	$\eta = 30\%$ $\epsilon = 30\%$
Battery	$w_{battery} = 1000\frac{Wh}{kg}$	$\eta = 99\%$

Tab. 1: Component assumptions for electric powertrain

Fig. 8 displays the “optimum” degree of hybridization with a variation of the design range.

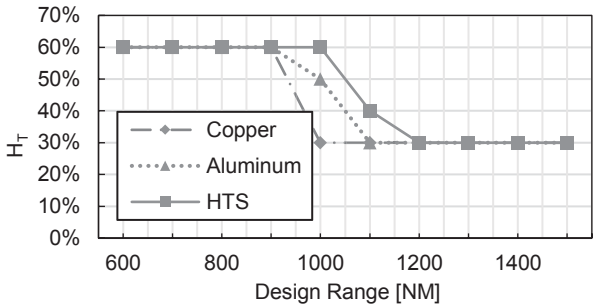

Fig. 8: Degree of hybridization for range variation and different conductor materials

Three conductor materials, aluminum, copper, and HTS are investigated. It should be noted that the degree of hybridization was not mathematically optimized. Instead, from a design of experiments, the best points with respect block fuel consumption were chosen manually.

The change in block fuel consumption compared to the conventional reference aircraft is shown in Fig. 9.

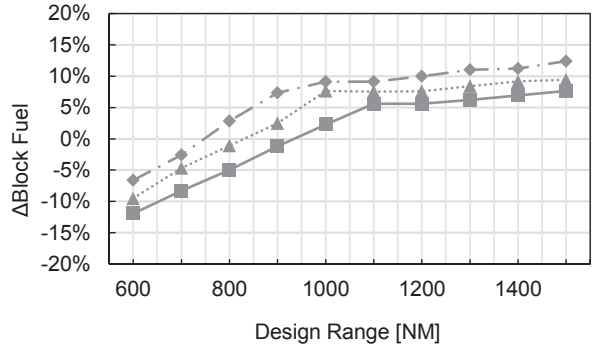

Fig. 9: Block fuel change for range variation and different conductor materials

The figure illustrates that a block fuel reduction is only achieved for design ranges below 900 NM for HTS conductors and for ranges below 800 NM and 730 NM for aluminum and copper respectively. The results also suggest that HTS is preferable to Aluminum and Copper. Considering conventional conducting materials, Aluminum leads to a lower block fuel than Copper, which is due to its lower gravimetric density. This shows that conductor efficiency seems to be less influential than its weight.

Since fuel is only one of two energy sources, the additional energy provided by the batteries has to be accounted too. In order to combine both energy forms in a single parameter, the so-called energy-specific air range (ESAR) is used. ESAR is defined as the mission range divided by the required mission energy

$$ESAR = \frac{Range\ [NM]}{E_{mission}\ [kWh]} \tag{15}$$

where the mission energy is the sum of the energy provided by batteries and fuel

$$E_{mission} = m_{blockFuel} \cdot LHV_{fuel} + E_{battery} \quad (16)$$

with LHV_{fuel} as the lower heating value of the fuel. In Fig. 10 it can be seen that the ESAR for the hybrid electric aircraft is lower compared to the conventional reference at all considered design ranges and for all of the three conducting materials. HTS again appears to be the preferable conducting technology (c.f. Fig. 9).

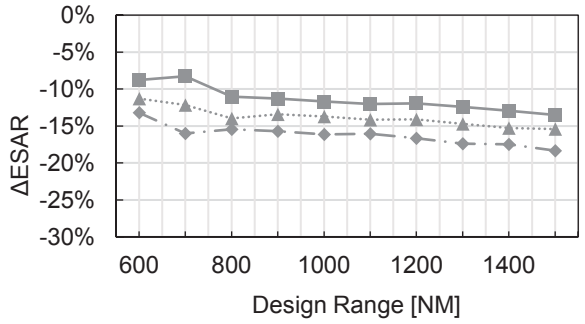

Fig. 10: Change in ESAR for range variation and different conducting materials.

The ESAR reduction for the hybrid electric version is equivalent to an increase in total required mission energy. This becomes plausible on closer examination of the mass changes resulting from the sizing process within MICADO shown in Fig. 11.

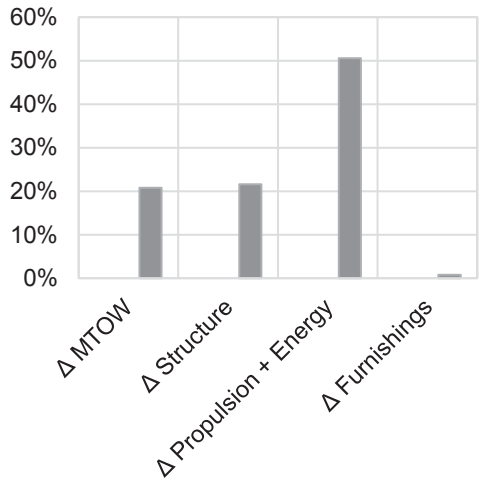

Fig. 11: Mass changes for the hybrid electric aircraft. Design range: 1000 NM, H_T: 30%

The MTOW of the hybrid electric aircraft is about 20% higher than that of the reference configuration. The main contributor to this is the additional mass of the electric powertrain. The additional structural weight results from snowball effects in the sizing loop. This is highlighted in more detail in the aircraft mass breakdown for the two configurations shown in Fig. 12.

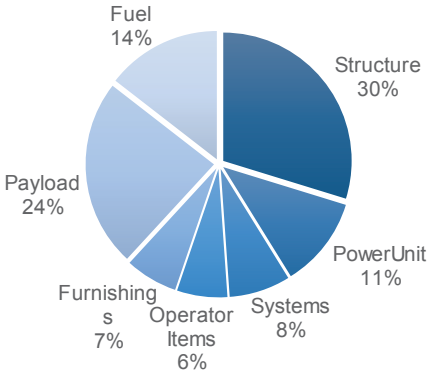

a): Mass breakdown of the conventional aircraft (MTOW)

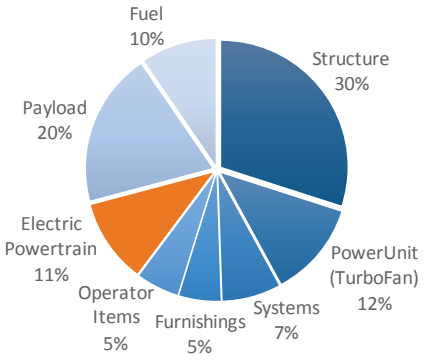

a): Mass breakdown of the hybrid electric aircraft (MTOW). Hybridization H_T: 30%

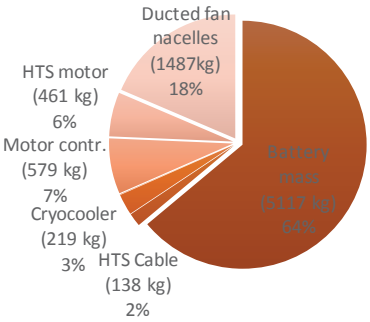

b): Component mass breakdown of the electric powertrain

Fig. 12: Mass breakdown of the two aircraft configurations. Design range 1000 NM

It can be seen from Fig. 12 a) that the electric powertrain with a total mass of about 8000 kg accounts for 11% of the MTOW. The majority (64%) of this is due to the large battery mass of more than 5000 kg. This again underlines the great influence of the battery technology on the feasibility of electric propulsion concepts as one of the major bottlenecks.

5.2. Influence of electric powertrain components on the hybrid electric aircraft

In the previous section, the most influential components on the overall powertrain mass breakdown were highlighted. Due to the fact that some assumptions had to be made for

the design of these components, their sensitivities are being examined in more detail for the overall system in this section. Fig. 14 displays the influence of specific component weights on the overall aircraft, deviating the specific component weights from the reference values in section 5.1.

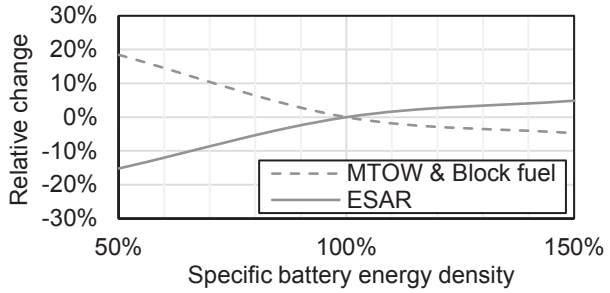

a) Battery

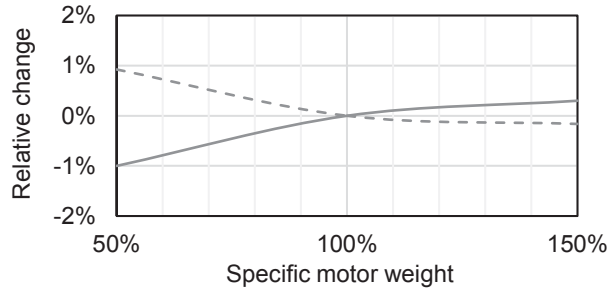

b) Electric motor

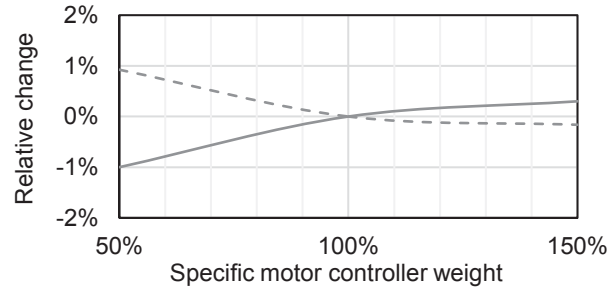

c) Motor controller

Fig. 13: Sensitivities for specific component weights

While in the figure, only battery, electric motor and motor controller are shown in detail, the sensitivity studies were carried out for all components of the electric powertrain. However, since these components have a relatively small share in the mass breakdown, their influence on the overall aircraft is rather small and is therefore not shown here. As expected, the battery specific energy density has the largest influence on the MTOW and ESAR. A variation of -50% reducing the specific energy density to 500 Wh/kg already decreases ESAR by 15% and increases MTOW by 18%. On the other hand, an increase in specific energy density of 50% (1500 Wh/kg) only increases ESAR by 5% and decreases MTOW by 5%. This again shows the occurrence of snowball effects due to the large increase in individual masses. The specific motor and motor controller weight variations show a similar curve in the diagram. However the influence on the overall aircraft compared to the battery is relatively small, highlighting again the large influence of the energy storage technology.

6. CONCLUSION AND OUTLOOK

As for now, it appears that for the selected hybrid propulsion architecture, no reduction in mission energy can be achieved. This is not very surprising, as for reasons of simplicity, in the presented systems architecture, the additional set of engines result in a significant increase of overall aircraft weight. However, the block fuel reduction for design ranges below 900 NM would in turn result in an decrease of exhaust emissions on aircraft level. As an outlook to future work, some of the main research priorities derived from the studies in this paper are listed below.

Firstly, the propulsion concept itself has to be revised. Under consideration of a different hybrid system architecture, a decrease in total energy demand for the mission is conceivable. Finding the right architecture for the specific use-case is definitely one of the main tasks when aiming towards overall efficiency. While the most pragmatic approach with regard to implementation was taken in this work, future investigations have to focus more on the potential to decrease the total mission energy demand. Possible investigations can include distributed electric propulsion concepts, enabling synergies between the propulsion and the aerodynamic performance of the aircraft. Secondly, a critical view on the TLAR is required. It is possible that aircraft of the A320 class are simply not suitable for hybrid electric propulsion. Possibly, smaller aircraft with less payloads and lower cruise speeds have a higher potential. Additionally, some of the assumptions made in this work have to be revised critically. While studies by Pornet et al. predicted a block fuel reduction for ranges below 1000 NM for a similar systems architecture, within this work, this could only be shown for rages below 900 NM. Possible improvements include for instance the applied ducted fan model. Furthermore, in the current setup, the degree of hybridization was kept at a constant value throughout the mission. In the future, an optimized hybridization for each mission segment could be applied. Besides, the assumed minimum state of charge for the battery of 20% has a large influence on the battery mass. Therefore, an improvement of battery enabling a full discharge would additionally improve results.

Taking all the achieved results into account, as a conclusion, it can be stated that the applied architecture serves as a feasible starting point for hybrid electric propulsion concepts for large aircraft at ILR and paves the way for future investigations in the field.

BIBLIOGRAPHY

[1] European Commission: Flightpath 2050. Europe's Vision for Aviation. Maintaining Global Leadership & Serving Society's Needs. Report of the High-Level Group on Aviation Research. Policy / European Commission, Luxembourg: Publications Office of the European Union, ISBN 978-92-79-19724-6, 2011.

[2] Risse, K.; Anton, E.; Lammering, T.; Franz, K.; Hoernschemeyer, R.: An Integrated Environment for Preliminary Aircraft Design and Optimization. In: 53rd AIAA/ASME/ASCE/AHS/ASC Structures, Structural Dynamics and Materials Conference, AIAA SciTech, American Institute of Aeronautics and Astronautics, AIAA 2012-1675, 2012.

[3] Bradley, M. K.; Droney, C. K.; Allen, T. J.: Subsonic Ultra Green Aircraft Research. Phase II - Volume II - Hybrid Electric Design Exploration. NASA/CR–2015-218704/Volume II, 2015.

[4] Airbus Group: E-Thrust. Electrical distributed propulsion system concept for lower fuel consumption, fewer emissions and less noise, 2018.

[5] Hornung, M.; Isikveren, A. T.; Cole, M.; Sizmann, A.: Ce-Liner - Case Study for eMobility in Air Transportation. In: 2013 Aviation Technology, Integration, and Operations Conference, AIAA Aviation Forum, American Institute of Aeronautics and Astronautics, 2013.

[6] Pornet, C.; Gologan, C.; Vratny, P. C.; Seitz, A.; Schmitz, O.; Isikveren, A. T.; Hornung, M.: Methodology for Sizing and Performance Assessment of Hybrid Energy Aircraft. Journal of Aircraft, Vol. 52, No. 1, pp. 341–352, 2015.

[7] Pornet, C.: Electric Drives for Propulsion System of Transport Aircraft. In: New Applications of Electric Drives. InTech, ISBN 978-953-51-2233-3, 2015.

[8] Pornet, C.; Isikveren, A. T.: Conceptual design of hybrid-electric transport aircraft. Progress in Aerospace Sciences, Vol. 79, pp. 114–135, 2015.

[9] Bijewitz, J.; Seitz, A.; Isikveren, A. T.; Hornung, M.: Multi-disciplinary design investigation of propulsive fuselage aircraft concepts. Aircraft Engineering and Aerospace Technology, Vol. 88, No. 2, pp. 257–267, 2016.

[10] Seitz, A.: H2020 CENTRELINE – Project Preview. 7th EASN International Conference, 2017.

[11] Vratny, P. C.; Gologan, C.; Pornet, C.; Isikveren, A. T.; Hornung, M.: Battery Pack Modeling Methods for Universally-Electric Aircraft. In: 4th CEAS Air & Space Conference, 2013.

[12] National Academies of Sciences, Engineering, and Medicine: Commercial Aircraft Propulsion and Energy Systems Research. Reducing Global Carbon Emissions, Washington, D.C: The National Academies Press, ISBN 978-0-309-44096-7, 2016.

[13] Stückl, S.; van Toor, J.; Lobentanzer, H.: VOLTAIR-the all electric propulsion concept platform-a vision for atmospheric friendly flight. In: 28th congress of the International Council of the Aeronautical Sciences, International Council of the Aeronautical Sciences, 2012.

[14] Felder, J. L.: NASA Electric Propulsion System Studies, 2015.

[15] Felder, J. L.; Kim, H. D.; Brown, G. V.: Turboelectric distributed propulsion engine cycle analysis for hybrid-wing-body aircraft. In: 47th AIAA Aerospace Sciences Meeting including the New Horizons Forum and Aerospace Exposition, 2009.

[16] Welstead, J.; Felder, J. L.; Guynn, M.; Haller, B.; Tong, M.; Jones, S.; Ordaz, I.; Quinlan, J.; Mason, B.: Overview of the NASA STARC-ABL (Rev. B) Advanced Concept, 2017.

[17] Moore, M. D.: Distributed Electric Propulsion (DEP) Aircraft, 2012.

[18] Lammering, T.; Schneider, T.; Stumpf, E.: The Right Single-Aisle for the Future Market. In: 53rd AIAA Aerospace Sciences Meeting 2015, AIAA SciTech, American Institute of Aeronautics and Astronautics, AIAA 2015-1900, 2015.

[19] Thielmann, A.; Neef, C.; Hettesheimer, T.; Döscher, H.; Wietschel, M.; Tübke, J.: Energiespeicher-Roadmap (Update 2017) - Hochenergiebatterien 2030+ und Perspektiven zukünftiger Batterietechnologien, 2017.

[20] Coordinating Research Council: Handbook of Aviation Fuel Properties. CRC Report No. 530, 1983.

[21] PolyPlus: PolyPlus Press Kit. Vol. 3, 2017.

[22] Stückl, S.: Methods for the Design and Evaluation of Future Aircraft Concepts Utilizing Electric Propulsion Systems. Technische Universität München, PhD thesis, 2015.

[23] Kasikci, I.: Planung von Elektroanlagen. Theorie, Vorschriften, Praxis, Berlin, Heidelberg: Springer Vieweg, ISBN 9783642409707, 2015.

[24] Willén, D.; Hansen, F.; Däumling, M.; Rasmussen, C. N.; Østergaard, J.; Træholt, C.; Veje: First operation experiences from a 30 kV, 104 MVA HTS power cable installed in a utility substation. Physica C: Superconductivity and its Applications, Vol. 372-376, pp. 1571–1579, 2002.

[25] Xi, H. X.; Gong, W. Z.; Zhang, Y.; Bi, Y. F.; Ding, H. K.; Wen, H.; Hou, B.; Xin, Y.: China's 33.5m, 35kV/2kA HTS ac power cable's operation in power grid. Physica C: Superconductivity and its Applications, Vol. 445-448, pp. 1054–1057, 2006.

[26] Haugan, T. J.; Long, J. D.; La Hampton: Design of compact, lightweight power transmission devices for specialized high power applications. SAE International Journal of Aerospace, Vol. 1, 2008-01-2930, pp. 1088–1094, 2008.

[27] Wang, B.: Siemens and Emrax claim best power to weight ratio for electric motors in the 5 to 10 kilowatt per kg range. https://www.nextbigfuture.com/2015/04/siemens-and-emrax-claim-best-power-to.html (accessed August 02, 2018), 2015.

[28] EMRAX: EMRAX 268 / 268 VHML Technical Data Table, 2015.

[29] Siemens: Factsheet - Rekord-Motor SP260D und Extra 330LE, 2015.

[30] Vogt, K.; Muller, G.: Elektrische Maschinen. Eine Einführung, Technik Berlin, ISBN 978-3527405251, 2007.

[31] Brown, G. V.: Weights and Efficiencies of Electric Components of a Turboelectric Aircraft Propulsion System. In: 49th AIAA Aerospace Sciences Meeting including the New Horizons Forum and Aerospace Exposition, 2011.

[32] Sivasubramaniam, K.; Zhang, T.; Lokhandwalla, M.; Laskaris, E. T.; Bray, J. W.; Gerstler, B.; Shah; Alexander, J. P.: Development of a high speed HTS generator for airborne applications. IEEE

Transactions on Applied Superconductivity, Vol. 19, No. 3, pp. 1656–1661
[33] Radebaugh, R.: Cryocoolers for aircraft superconducting generators and motors. In: Advances in Cryogenic Engineering: Transactions of the Cryogenic Engineering Conference, American Institute of Physics, Vol. 1434, Issue 1, 2012.
[34] Seitz, A.: Advanced methods for propulsion system integration in aircraft conceptual design. Technische Universität München, PhD thesis, 2012.
[35] GasTurb GmbH: GasTurb 12. Design and Off-Design Performance of Gas Turbines. User manual, 2015.
[36] Berg, F.; Palmer, J.; Miller, P.; Dodds, G.: HTS System and Component Targets for a Distributed Aircraft Propulsion System. In: IEEE Transactions on Applied Superconductivity, ISBN 1051-8223, pp. 1–7, 2017.
[37] Palmer, J.; Shehab, E.: Modelling of cryogenic cooling system design concepts for superconducting aircraft propulsion. IET Electrical Systems in Transportation, Vol. 6, No. 3, pp. 170–178, 2016.
[38] ter Brake, H.J.M.; Wiegerinck, G.F.M.: Low-power cryocooler survey. Cryogenics, Vol. 42, No. 11, pp. 705–718, 2002.
[39] Pop, V.; Bergveld, H. J.; Danilov, D.; Regtien, P.P.L.; Notten, P.H.L.: Battery management systems. Accurate state-of-charge indication for battery-powered applications, Springer, ISBN 1-402-06944-8, 2008.